

***In vivo* Morphogenesis of a New Porcine Enteric Coronavirus, CV 777**

By

R. DUCATELLE¹, W. COUSSEMENT¹, M. B. PENSART²,
P. DEBOUCK², and J. HOORENS¹

Departments of Pathology¹ and Virology², Faculty of Veterinary Medicine,
State University of Gent, Gent, Belgium

With 9 Figures

Accepted November 20, 1980

Summary

The morphogenesis of a new porcine enteric coronavirus, CV777, in intestinal epithelial cells of experimentally infected newborn piglets is described. The virus shows a morphogenetic pattern characteristic for members of the Coronaviridae family. It is formed by budding through membranes of the endoplasmic reticulum. Some specific aspects of this morphogenesis are discussed.

Introduction

In 1978, a new coronavirus-like agent (CVLA), was demonstrated in the faeces of piglets from outbreaks of diarrhoea (16).

The clinical findings after natural and experimental infection have been described (7). The virus has been provisionally classified as a coronavirus, based on its morphologic aspect with negative staining. It has been shown to differ serologically from other known porcine coronaviruses, transmissible gastro-enteritis virus (TGEV) and haemagglutinating encephalo-myelitis virus (HEV) (16).

The pathogenesis of the experimental oronasal infection has been studied by immunofluorescence (8). The accompanying histological and ultrastructural lesions will be reported elsewhere (4, 11). The results of these studies show that virus replication occurs in the cytoplasm of absorptive epithelial cells covering the small intestinal villi and the large intestine. The intracellular virus replication results in alterations of cellular organelles and cell desquamation.

The present study deals with the morphogenesis of the CVLA in the intestinal epithelial cells of piglets after experimental oronasal infection.

Materials and Methods

Sixteen caesarean-derived colostrum-deprived piglets were inoculated oronasally on the second or third day of life with 10⁴ pig infective doses of a virus stock, obtained

as described elsewhere (DEBOUCK *et al.*, to be published). One piglet was kept as a control. The pigs were sacrificed at different time intervals after the inoculation (12, 18, 24, 30, 32, 36, 38, 41, 48, 60, 72, 96 and 120 hours).

Tissues were collected from the duodenum, middle jejunum and colon as described elsewhere in more detail (DUCATELLE *et al.*, to be published). The specimens were fixed in 2 per cent paraformaldehyde, 2.5 per cent glutaraldehyde in 0.1 molar cacodylate buffer. Postfixation was done with 1 per cent OsO₄. The blocks were stained with uranylacetate dehydrated in acetone in a vacuum chamber and then embedded in Spurr medium. Semi-thin sections were stained with toluidine blue; ultra-thin sections were stained with lead citrate.

Results

In the watery phase of diarrhoea, numerous viral particles were detected in the sections of the small intestinal villi.

Occasionally, the particles were seen in close apposition to, and between the microvilli of uninfected cells. More frequently, rows of virus particles were seen between the microvilli of heavily infected cells (Fig. 1). These cells showed an

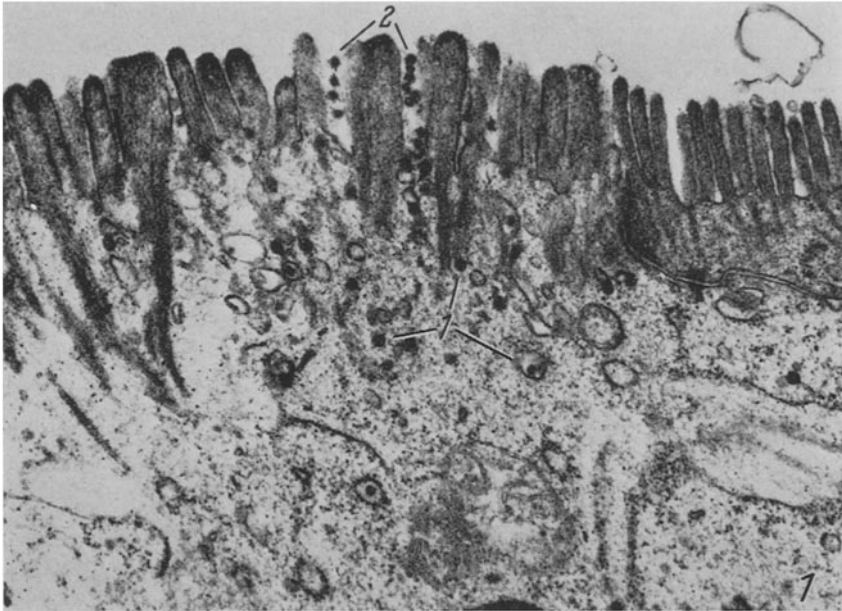


Fig. 1. Interaction of the virus with the apical cell membrane: 1 Viral particles in small cytoplasmic vesicles. 2 Rows of viral particles between the microvilli of an infected cell. $\times 23,275$; 36 hours post infection (hpi)

electron translucent cytoplasm and short, irregular microvilli. Cell free viral particles ranged in diameter from 60 to 90 nm. They were round and consisted of an inner electron dense core of 40 to 70 nm. This core sometimes showed a central clearing halo, but was completely electron-dense in other particles. It was separated by a narrow translucent ring from an outer unit-membrane.

Virions were sometimes seen in the intercellular space between epithelial cells. They were frequently present inside caveolae or apical pits between the microvilli

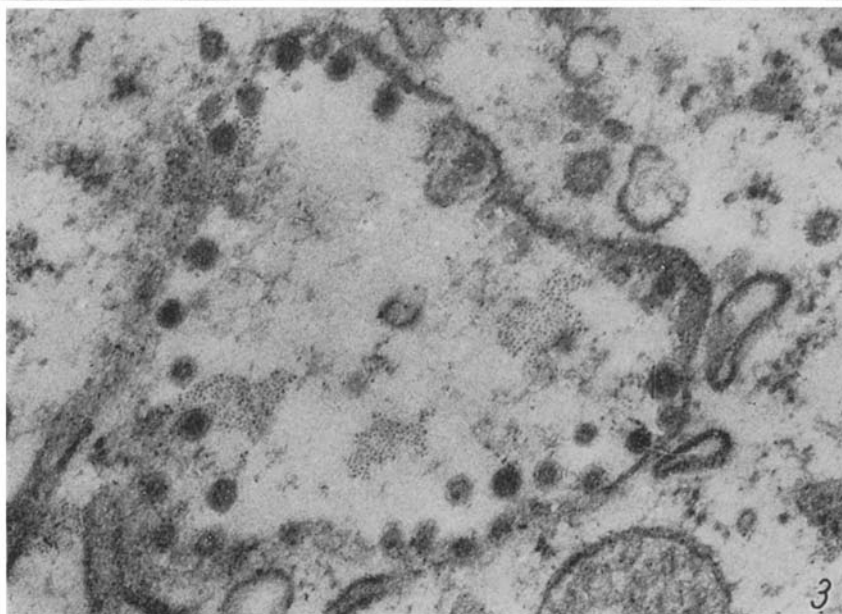
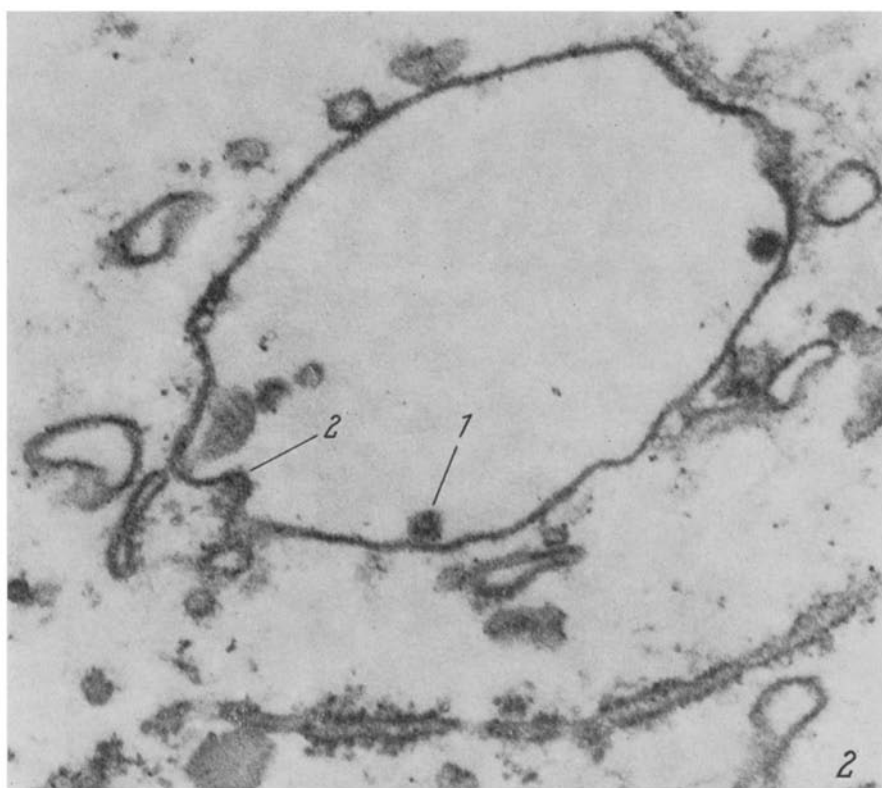


Fig. 2. Phenomena suggesting virus assembly: 1 Virus inside intracytoplasmic vacuole, in close apposition to the membrane. 2 Bud-like structure. $\times 68,600$; 24 hpi

Fig. 3. Phenomena suggesting virus assembly: Virus particles in close apposition to and superimposed on a vesicle membrane. $\times 68,600$; 24 hpi

of infected cells. They were also frequently observed inside small cytoplasmic vesicles in the terminal web area and in the apical cytoplasm. A small vesicle usually contained only one to two complete viral particles.

Virus maturation by budding through cytoplasmic membranes into cisternae of the smooth endoplasmic reticulum was occasionally seen (Fig. 2). Rows of viral particles were sometimes observed lining the membrane of large cytoplasmic vacuoles (Fig. 3). Some of these particles seemed to be superimposed on, or adhering to the membrane, which was often not clearly defined (Fig. 3). Many of these large cytoplasmic vacuoles were completely filled-up with viral particles. In some of the cytoplasmic vacuoles, annular structures were seen, resembling the outer viral membrane without an inner core.

A number of other large cytoplasmic vacuoles was filled with granulofibrillar material. They also contained virus particles at the inside of their membrane (Fig. 4).

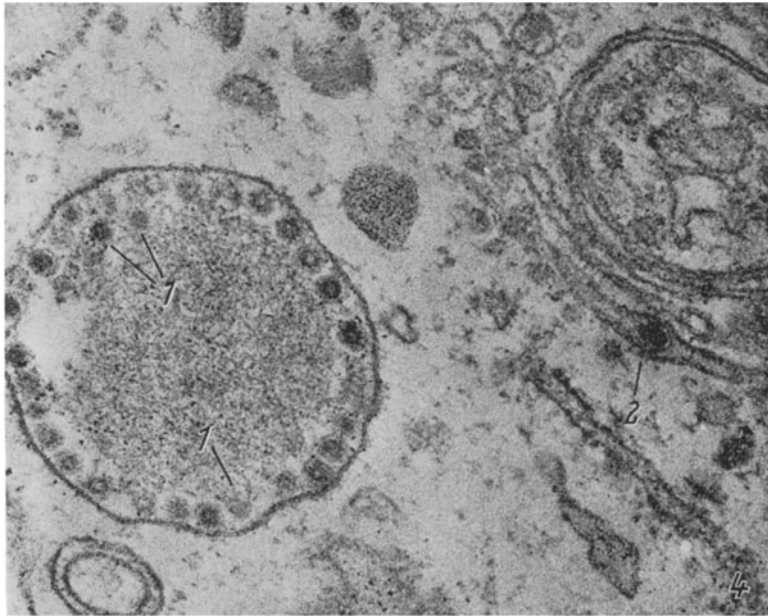


Fig. 4. Viral particles at the periphery of a vacuole (1), filled with electron dense granulo-fibrillar material. 2 Virus particle inside a Golgi sac, causing a spindle shaped distention of the lamellae. $\times 68,600$; 24 hpi

Another type again of large vacuoles showed a highly electron dense matrix with scattered viral particles. Some of these vacuoles had constrictions suggesting that one or two viral particles were separated from the vacuole.

Occasionally, bud-like structures were seen inside membranous whorls. Budding of viral particles at the cell membrane was never observed.

Strands of endoplasmic reticulum (EPR) sometimes contained rows of viral particles (Fig. 5). Viruses were often present within the Golgi sacs causing a spindle shaped distention of these lamellae (Fig. 4). Occasionally, the viral particles were seen inside the extremities of the Golgi saccules. In that case, the Golgi

lamellae sometimes showed a constriction next to the viral particle (Fig. 6). Small cytoplasmic vesicles containing one viral particle were frequently present in the Golgi area.

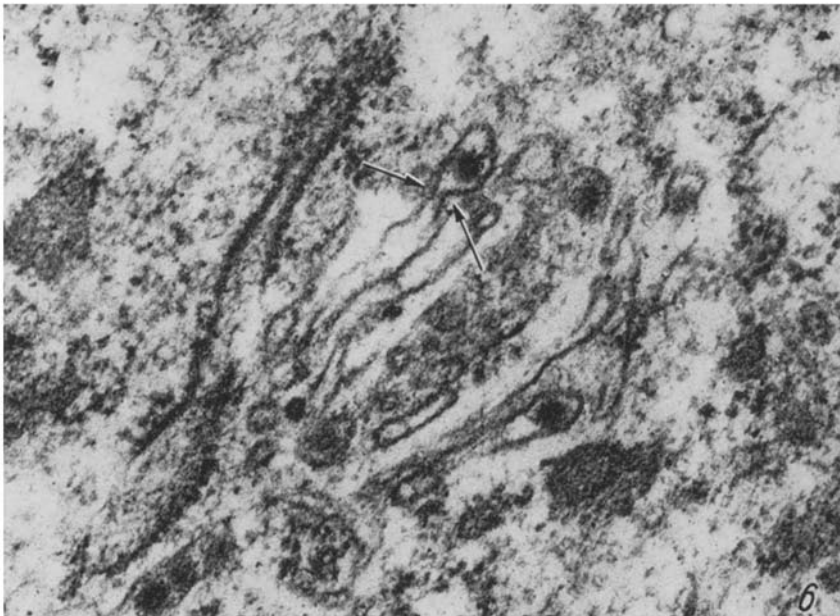
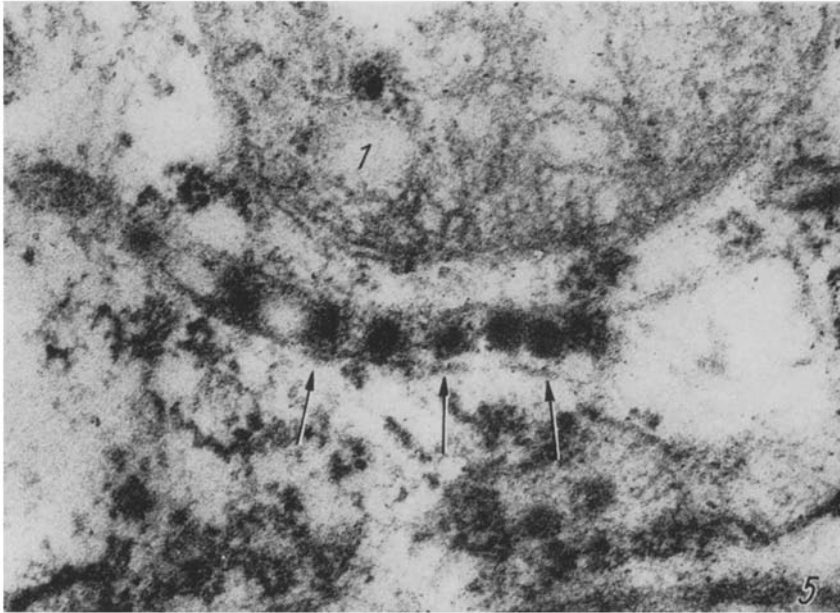


Fig. 5. Row of viral particles between the lamellae of the EPR (arrows). 1 Mitochondrion. $\times 86,800$; 120 hpi

Fig. 6. Virus particles present inside the extremities of the Golgi sacs, one particle appears to be in the process of "pinching-off" (arrows). $\times 68,600$; 96 hpi

The apical cytoplasmic membrane of heavily infected cells was sometimes ruptured with loss of cytoplasmic contents into the intestinal lumen. Viral particles were also sometimes observed inside desquamated epithelial cells in the gut lumen.

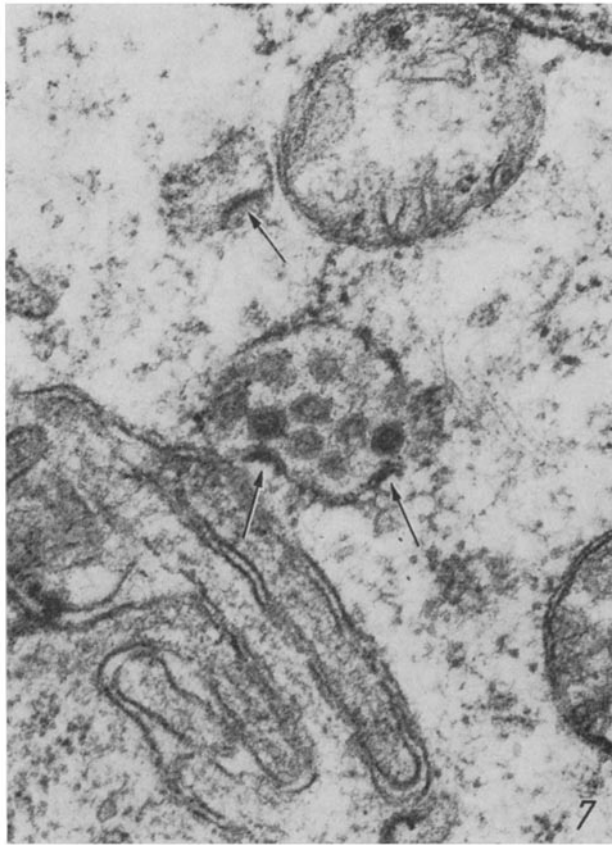


Fig. 7. Virus assembly by budding through EPR membranes: Arrows indicate virus crescents. $\times 68,600$; 122 hpi, 96 hours after the first clinical symptoms

Viral particles were never detected in the nuclei of epithelial cells. This morphogenetic pattern was seen in pigs killed at different stages of disease. It was most prominent in the pig killed 6 hours after the onset of diarrhoea. In later stages however, the number of large virus-containing vacuoles decreased and viral particles were observed more frequently between lamellae of the EPR, inside Golgi sacs, and in small cytoplasmic vesicles.

Nevertheless, in the piglet killed 96 hours after the onset of diarrhoea, when severely dehydrated and moribund, some particular observations were made:

Budding of viral particles through membranes of EPR was very commonly observed in this animal (Fig. 7). These budding structures ranged from early

creascent through particles in the middle of the budding process (Fig. 8) to viral particles linked to the membrane by only a narrow membranous bridge (Fig. 9).

Large cytoplasmic vacuoles with virus particles were now rarely seen. The particles were generally confined to dilated cisternae of EPR and to the Golgi sacs. The other aspects of the morphogenesis were similar to those observed during the watery phase of diarrhoea.

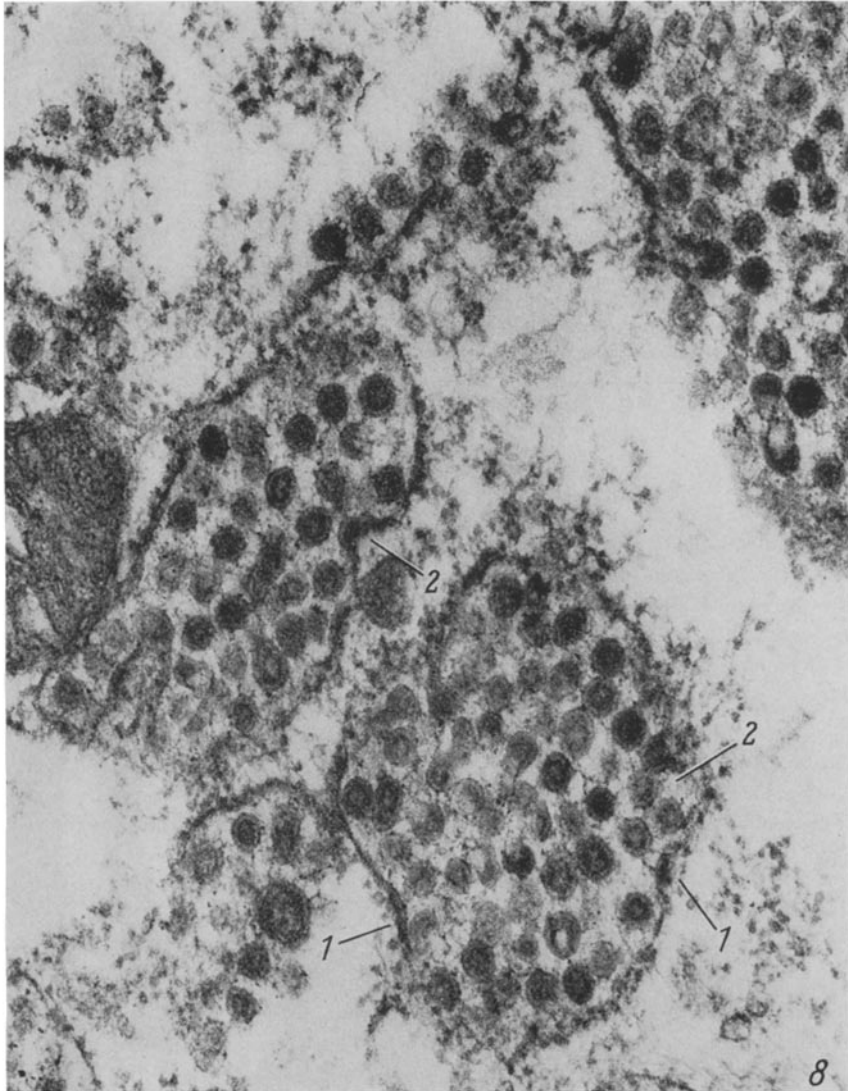


Fig. 8. Virus assembly by budding through EPR membranes: 1 Early "crescent" formation. An electron dense layer is formed parallel to the membrane. 2 Later stage, showing bulging of material into the EPR cisterna. $\times 70,000$; 96 hours after the first clinical symptoms

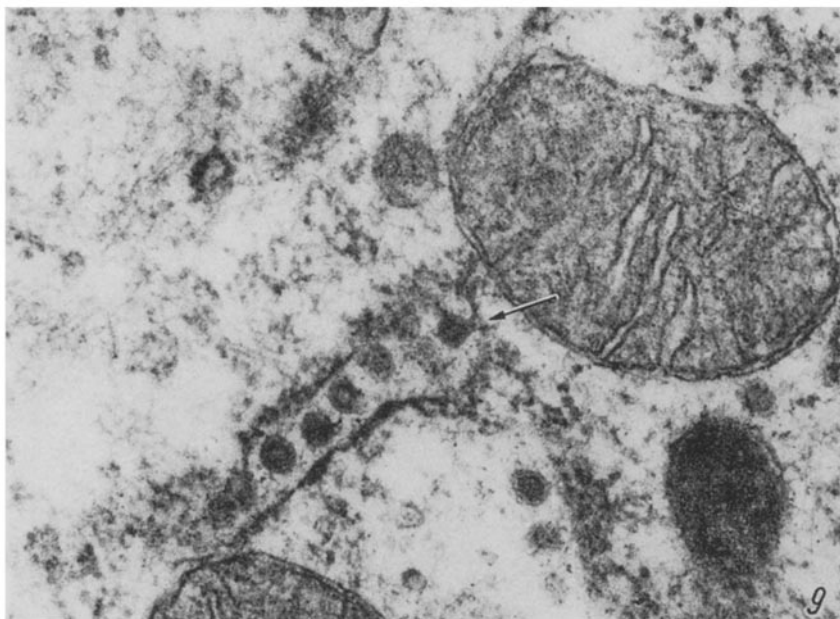


Fig. 9. Virus assembly by budding through EPR membranes: Arrow indicates a late bud, with the virus still linked to the membrane by a narrow bridge. $\times 68,000$; 96 hours after the first clinical symptoms

Discussion

A definite answer could not be obtained concerning the mode of uptake of the virus by the epithelial cells. Close apposition of virions to the apical cytoplasmic membrane of uninfected cells, as seen in the present study, has also been observed with TGEV (15).

The rows of viral particles between the microvilli of infected cells, and the viral particles present in apical pits, may represent either uptake or release of the virus. However, since their presence was often associated with heavy infection and morphologic alterations of the cell, it points to release rather than to uptake.

Assembly of the virus seems to occur by budding through intracytoplasmic membranes. Budding structures have been described in a number of coronaviral infections (1, 2, 13, 17, 19), and are considered to be characteristic for members of the family Coronaviridae (20). The frequency with which budding structures are observed seems to vary markedly not only from one coronavirus to the other (1, 12), but it also seems to depend on the host or cell type. This was very obvious in neonatal calf diarrhoea coronavirus (NCD CV) infection (2, 9). In the present study, budding structures were very frequently seen in the one animal killed 96 hours after the first clinical signs appeared, whereas they were very rarely observed in the earlier phases of diarrhoea when larger numbers of intracellular viral particles were present. The ultrastructure of the epithelial cells (DUCATELLE *et al.*, to be published) and the time delay between inoculation and euthanasia in this one animal indicate that these cells are a second generation of epithelial cells since the infection first started. Immunofluorescence of the intestine of this animal has

demonstrated that the cells are heavily infected (DEBOUCK *et al.*, to be published), whereas histopathological study has shown very little desquamation (COUSSEMENT *et al.*, to be published). All this may indicate that the virus assembly occurs slower in this second generation of infected epithelial cells than in the first generation, so that it is more easily observed by electron microscopy. The presence of many viral particles in close apposition to intracytoplasmic membranes of vacuoles, as described during the watery phase of diarrhoea, may indicate that these viral particles have just been passing through the process of budding. This also indicates that in the first generation of infected epithelial cells virus assembly is a rapid process. Structures resembling those called "viral factories" in NCDCV infection (10) have also been observed in cells infected with CVLA (Fig. 5). It can, however, not be excluded that they merely represent particles which came into these vesicles by budding through the membrane.

Membranous whorls, resembling the so-called "condensed tubular network" were also observed in the present material. It has been suggested that they represent some form of virus assembly (6, 14). The large, virus-containing intracytoplasmic vacuoles probably represent dilated cisternae of EPR (1). Since there exists a physiologic transport mechanism from the EPR to the Golgi apparatus (5), it is very possible that viral particles are transported to the Golgi cisternae, where they were frequently located. Golgi sacs have been reported as a site of morphogenesis of other coronaviruses (15, 19). Constrictions seen at the ends of the Golgi sacs and in electron dense cytoplasmic vacuoles (Fig. 6 and 8) suggest the pinching-off of small vesicles containing one or two viral particles. The numerous intravesicular particles seen in the cytoplasm of infected cells are probably produced in this way.

Similar small virus-containing vesicles have also been observed in other coronaviral infections (10, 15). Viral particles between the microvilli of heavily infected cells may originate from fusion of small virus-containing vesicles with the cell membrane. Fusion of small virus-filled vesicles with cell membranes has been described in human (3) and calf (18) coronaviral infections. The size and morphology of this CV777 virus and its intracellular development are in accordance with those reported for other coronaviridae (20). The average particle diameter in ultra-thin sections was however less than that described after negative staining (16). This discrepancy has also been observed in human coronaviruses (1), and is attributed to tissue shrinkage.

Acknowledgements

This study was supported by "Institut tot aanmoediging van het Wetenschappelijk Onderzoek in Nijverheid en Landbouw (IWONL-Brussels). We thank J. P. Logghe for ultramicrotome preparations and photography. We are indebted to the department of Virology (Dir. Prof. Pensaert) for preparing the infectious material.

References

1. BECKER, W. B., MCINTOSH, K., DEES, J. H., CHANOCK, R. M.: Morphogenesis of Avian Infectious Bronchitis virus and a related human strain (strain 229E). *J. Virol.* **1**, 1019—1027 (1967).
2. BRIDGER, J. C., CAUL, E. O., EGGLESTONE, S. I.: Replication of an enteric bovine coronavirus in intestinal organ cultures. *Arch. Virol.* **57**, 43—51 (1978).

3. BUCKNALL, R. A., KALICA, A. R., CHANOCK, R. M.: Intracellular development and mechanism of hemadsorption of a human coronavirus, OC43. *Proc. Exp. Biol. Med.* **139**, 811—817 (1972).
4. COUSSEMENT, W., DUCATELLE, R., DEBOUCK, P., HOORENS, J.: Pathology of experimental CV777 coronavirus enteritis in piglets. 1) Histological and histochemical study. *Veterinary Pathology* (to be published).
5. DAVID, H.: Ortho- and pathomorphology of human and animal cells in drawings, diagrams and constructions, 1st ed., 128. Stuttgart: Gustav Fischer Verlag 1978.
6. DAVID-FERREIRA, J. F., MANAKER, R. A.: An electron microscopic study of the development of a mouse hepatitis virus in tissue culture cells. *J. Cell. Biol.* **24**, 57—78 (1965).
7. DEBOUCK, P., Pensaert, M. B.: Experimental infection of pigs with a new porcine enteric coronavirus, CV777. *Amer. vet. Res.* **41**, 219—223 (1980).
8. DEBOUCK, P., Pensaert, M., COUSSEMENT, W.: The pathogenesis of an enteric infection in pigs, experimentally induced by the coronavirus-like agent, CV777. *Veterinary Microbiology* (to be published).
9. DOUGHRI, A. M., STORZ, J., HAJER, I., FERNANDO, H. S.: Morphology and morphogenesis of a coronavirus infecting intestinal epithelial cells of newborn calves. *Expt. mol. Pathol.* **25**, 355—370 (1976).
10. DOUGHRI, A. M., STORZ, J.: Light and ultrastructural pathologic changes in intestinal coronavirus infection of newborn calves. *Zbl. Vet. Med. B* **24**, 367—385 (1977).
11. DUCATELLE, R., COUSSEMENT, W., DEBOUCK, P., HOORENS, J.: Pathology of experimental CV777 coronavirus enteritis in piglets: 2) Electron microscopic study. *Veterinary Pathology* (to be published).
12. HAMRE, D., KINDIG, D. A., MANN, J.: Growth and intracellular development of a new respiratory virus. *J. Virol.* **1**, 810—816 (1967).
13. McINTOSH, K.: Coronaviruses: A comparative review. *Curr. Top. Microbiol. Immunol.* **63**, 84—129 (1974).
14. OSHIRO, L. S., SCHIEBLE, J. H., LENNETTE, E. H.: Electron microscopic studies of coronavirus. *J. gen. Virol.* **12**, 161—168 (1971).
15. Pensaert, M., Haelterman, E. O., Hinsman, E. J.: Transmissible Gastroenteritis of swine: virus-intestinal cell interactions. II. Electron microscopy of the epithelium in isolated jejunal loops. *Arch. ges. Virusforsch.* **31**, 335—351 (1970).
16. Pensaert, M., DEBOUCK, P.: A new coronavirus-like particle associated with diarrhea in swine. *Arch. Virol.* **58**, 243—247 (1978).
17. PEDERSEN, N. C.: Morphologic and physical characteristics of Feline Infectious Peritonitis virus and its growth in autochthonous peritoneal cell cultures. *Amer. J. vet. Res.* **37**, 567—572 (1976).
18. STORZ, J., DOUGHRI, A. M., HAJER, I.: Coronaviral morphogenesis and ultrastructural changes in intestinal infections of calves. *J. A. V. M. A.* **173**, 633—635 (1978).
19. TAKEUCHI, A., BINN, L. N., JERVIS, H. R., KEENAN, K. P., HILDEBRANDT, P. K., VALAS, R. B., BLAND, F. F.: Electron microscope study of experimental enteric infection in neonatal dogs with a canine coronavirus. *Lab. Invest.* **34**, 539—549 (1976).
20. TYRRELL, D. A. J., ALEXANDER, D. J., ALMEIDA, J. D., CUNNINGHAM, C. H., EASTERDAY, B. C., GARWES, D. J., HIERHOLZER, J. C., KAPIKIAN, A., MACNAUGHTON, M. R., McINTOSH, K.: Coronaviridae: Second report. *Intervirology* **10**, 321—328 (1978).

Authors' address: Dr. R. DUCATELLE, Department of Veterinary Pathology, Faculty of Veterinary Medicine, State University of Gent, Casinoplein 24, B-9000 Gent, Belgium.

Received September 15, 1980